

Instantons and the fixed point topological charge in the two-dimensional O(3) σ model

Marc Blatter, Rudolf Burkhalter, Peter Hasenfratz, and Ferenc Niedermayer*

Institut für Theoretische Physik, Universität Bern, Sidlerstrasse 5, CH-3012 Bern, Switzerland

(Received 6 September 1995)

We define a fixed point topological charge for the two-dimensional O(3) lattice σ model which is free of topological defects. We use this operator in combination with the fixed point action to measure the topological susceptibility for a wide range of correlation lengths. The results strongly suggest that it is not a physical quantity in this model. The procedure, however, can be applied to other asymptotically free theories as well.

PACS number(s): 11.15.Ha, 11.10.Hi, 75.10.Hk

I. INTRODUCTION

Topological effects play an important role in the dynamics of asymptotically free field theories. In QCD instantons may be responsible for breaking the axial symmetry resolving the so-called U(1) problem [1]. In a large N_c limit the topological susceptibility relates the masses of the pseudoscalars η , η' , and K [2].

The topological susceptibility χ_t may be defined as the infinite volume limit of

$$\chi_t^V = \frac{\langle Q^2 \rangle}{V}, \quad (1)$$

where Q is the topological charge and V is the space-time volume. In the two-dimensional O(3) nonlinear σ model it is a dimension two quantity that vanishes to all orders in the weak coupling expansion. From the perturbative renormalization group (RG) it is expected to scale according to the two-loop β function

$$\chi_t \propto \beta^2 \exp(-4\pi\beta) \quad (\beta \rightarrow \infty). \quad (2)$$

It is a nontrivial task to recover the correct continuum results from lattice Monte Carlo (MC) simulations. A lattice topological charge definition is needed, which returns even for large fluctuations reliable results.

A "geometric" definition proposed by Berg and Lüscher [3] is based on adding up the area of spherical triangles, which are defined by the spin vectors in an elementary plaquette. As the contributions from all plaquettes are summed up, the internal space — the sphere described by the spin variables — is covered, and if periodic boundary conditions are used one obtains an integer charge signifying the number of times this sphere is "wrapped." The topological susceptibility evaluated with this charge definition (and the standard action)

completely failed to scale [3–5]. The reason was ascribed to special configurations called "dislocations" [5], which are dominant in the statistical average. Dislocations are nonzero charged configurations whose contributions to the topological charge come entirely from small localized regions where they become "singular." If the minimal action of dislocations is smaller than the continuum value of a one-instanton configuration (i.e., 4π) then dislocations will dominate the path integral and spoil the scaling behavior, Eq. (2) [4,5].

Another definition goes back to DiVecchia *et al.* [6] — for a recent discussion including the fixed point (FP) action see Ref. [7]. It is called a field theoretical or plaquette definition and uses a "naive" discretization of the continuum charge operator. This prescription does not yield integer values, and to obtain continuum results renormalization factors are needed. For large β these factors can be determined perturbatively, but for intermediate β one has to use nonperturbative techniques [8–11]. Results obtained with the field theoretical charge indicate for the susceptibility a behavior consistent with scaling [9,11].

A serious problem in these approaches is the role of the lattice artifacts, sensitive both to the form of the lattice action and the choice of the topological charge. A recent work [13] suggests using the FP action of a renormalization-group transformation to study topological effects. In particular, an important feature is that the FP action has scale-invariant instanton solutions (with an action value exactly 4π), and hence — as will be discussed in this paper — one can define a topological charge with no lattice defects. In Ref. [13] and here the O(3) σ model is considered, but the methods apply to other asymptotically free theories as well. The SU(3) gauge theory has been studied in Refs. [14,15]. A subsequent paper by one of us [17], will deal with the application of these ideas to CP^{N-1} models and in particular to the CP^3 model. Some of our results were already presented in Ref. [16].

The paper is organized as follows: First we review some results derived in Ref. [13] and define the FP field operator. This is followed by a closer look at instantons in the continuum, in a finite periodic volume and finally on a lattice using the FP action. We then define the FP

*On leave from the Institute of Theoretical Physics, Eötvös University, Budapest, Hungary.

topological charge and present some numerical results on classical solutions. In the last section we analyze the topological susceptibility evaluated in a Monte Carlo simulation. After a brief description of the methods used, we present the results, which are followed by a conclusion and an outlook.

II. RG RESULTS AT THE CLASSICAL LEVEL

A. Review of the RG transformation and its fixed point

Let us briefly summarize some RG results, which were developed in a previous paper [13]. For a detailed discussion we refer the reader to this paper.

We consider the $O(3)$ nonlinear σ model in two-dimensional Euclidean space defined on a square lattice. The partition function reads as follows:

$$Z = \int DS e^{-\beta \mathcal{A}(\mathbf{S})}. \quad (3)$$

Here DS is the $O(3)$ invariant measure

$$DS = \prod_n d^3 S_n \delta(\mathbf{S}_n^2 - 1), \quad (4)$$

and $\beta \mathcal{A}(\mathbf{S})$ is a regularization of the continuum action

$$\beta \mathcal{A}_{\text{cont}}(\mathbf{S}) = \frac{\beta}{2} \int d^2x \partial_\mu \mathbf{S}(x) \partial_\mu \mathbf{S}(x), \quad \text{where } \mathbf{S}^2(x) = 1. \quad (5)$$

We perform exact RG transformations by a Kadanoff type of blocking; i.e., we divide the lattice into 2×2 blocks labeled by indices n_B . To each block we define a block spin variable \mathbf{R}_{n_B} , which is some mean of the spin variables \mathbf{S}_n in the block. The block spins \mathbf{R}_{n_B} form a lattice whose spacing is twice as large as the original

one. An effective action is defined by integration over the original lattice:

$$e^{-\beta' \mathcal{A}'(\mathbf{R})} = \int DS e^{-\beta[\mathcal{A}(\mathbf{S}) + \mathcal{T}(\mathbf{R}, \mathbf{S})]}, \quad (6)$$

where \mathcal{T} is the kernel of the RG transformation, and its normalization

$$\int D\mathbf{R} e^{-\beta' \mathcal{T}(\mathbf{R}, \mathbf{S})} = 1 \quad (7)$$

ensures the invariance of the partition function under this transformation. In the classical limit ($\beta \rightarrow \infty$) the path integral is dominated by its saddle point:

$$\mathcal{A}'(\mathbf{R}) = \min_{\{\mathbf{S}\}} \{\mathcal{A}(\mathbf{S}) + \mathcal{T}(\mathbf{R}, \mathbf{S})\}. \quad (8)$$

The transformation kernel used in Ref. [13] has in the limit $\beta \rightarrow \infty$ the simple form

$$\mathcal{T}(\mathbf{R}, \mathbf{S}) = \kappa \sum_{n_B} \left(\left| \sum_{n \in n_B} \mathbf{S}_n \right| - \mathbf{R}_{n_B} \cdot \sum_{n \in n_B} \mathbf{S}_n \right). \quad (9)$$

Here κ is a free positive parameter of the RG transformation, which is tuned to make the FP action as compact as possible. As indicated by the free field theory in one dimension, the choice $\kappa = 2$ gives the most short-ranged FP action. A fixed point of the transformation satisfies the equation

$$\mathcal{A}_{\text{FP}}(\mathbf{R}) = \min_{\{\mathbf{S}\}} \{\mathcal{A}_{\text{FP}}(\mathbf{S}) + \mathcal{T}(\mathbf{R}, \mathbf{S})\}. \quad (10)$$

This equation, called the FP equation, fixes for arbitrary configurations $\{\mathbf{R}\}$ the value of the FP action. Starting from a lattice regularization of the continuum action, repeated RG transformations will drive the effective action to its fixed point. This takes on the form of a minimization in a multigrid of lattice configurations:

$$\mathcal{A}^{(k)}(\mathbf{R}) = \min_{\{\mathbf{S}^{(1)}, \mathbf{S}^{(2)}, \dots, \mathbf{S}^{(k)}\}} \left\{ \mathcal{A}^{(0)}(\mathbf{S}^{(k)}) + \mathcal{T}(\mathbf{S}^{(k)}, \mathbf{S}^{(k-1)}) + \dots + \mathcal{T}(\mathbf{R}, \mathbf{S}^{(1)}) \right\}. \quad (11)$$

On each successive level (see Fig. 1), the spin configurations become smoother, not only because the lattice spacing is halved, but also because the minimization tends to smooth out the fluctuations around a solution to the equations of motion. Hence, one may choose for the action $\mathcal{A}^{(0)}(\mathbf{S}^{(k)})$ on the finest configuration $\{\mathbf{S}^{(k)}\}$ any lattice discretization of the continuum action. The FP action \mathcal{A}_{FP} is then obtained as the limit of $k \rightarrow \infty$ of $\mathcal{A}^{(k)}(\mathbf{R})$. For practical purposes, however, only a few levels are needed, and starting from the standard action on the lowest level the FP value is reached soon.

B. Parametrization of the FP action

In principle, the above multigrid approach can be used to evaluate the FP action for arbitrary configurations to

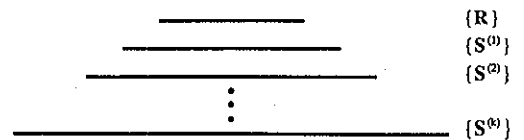


FIG. 1. A multigrid obtained by iterating the FP equation.

any precision desired. For practical calculations, however, a parametrization of the FP action is needed. In Ref. [13] a parametrization has been obtained by fitting the known values of the action for ~ 500 configurations. That parametrization represented the FP action well on those configurations. However, to control the topological effects better, we decided to improve the parametrization further by including some small size topological solutions in the fitting procedure. We used several two-instanton solutions of the lattice FP action. While improving the fit for these instanton solutions, the new parametrization does not affect the quality of the fit for the previous configurations.

The resulting couplings are given in Table I, together with a graphical notation of the corresponding operators. Let us explain here again the meaning of this notation. The parametrization of the action has the form

$$\mathcal{A}_{\text{FP}}(\mathbf{S}) = \sum \text{coupling} \times \text{products of } \frac{1}{2}\vartheta_{n_i, n_j}^2, \quad (12)$$

where ϑ_{n_i, n_j} is the angle between the two spins \mathbf{S}_{n_i} and \mathbf{S}_{n_j} . Two dots connected with a line $\bullet\text{---}\bullet$ represent a factor $\frac{1}{2}\vartheta_{n_i, n_j}^2$ in the action, and the positions of the dots represent the lattice sites n_i and n_j , respectively. Double (triple) connected dots stand for the square (cube) of the above factors. The operator, finally, is the product of all

the factors $\frac{1}{2}\vartheta_{n_i, n_j}^2$, as indicated by the lines in the figure. The quadratic and quartic couplings 1, 2, 4, 5, 7, 10, 16, and 19 are determined analytically [13]; the others are determined with a numerical fitting procedure with the new instanton configurations added.

C. The fixed point field

As we shall see in Sec. IIIB, FP operators are closely related to the FP field. The FP field is the fine field $\mathbf{S}^{(k)}$ in the multigrid solution of the iterated FP equation (11) as k goes to infinity. If the functional dependence of the solution on the first fine level $\mathbf{S}^{(1)}$ on \mathbf{R} is known, the FP field can be evaluated by iteration. Below we construct the operator $\mathbf{S}^{(1)} = \mathbf{S}^{(1)}(\mathbf{R})$. (In the limit $k \rightarrow \infty$ the solution $\{\mathbf{S}^{(1)}\}$ of the iterated FP equation is identical to the solution $\{\mathbf{S}\}$ of the FP equation.)

For smooth fields a quadratic approximation of the FP equation can be made, which can be solved analytically. Consider a smooth configuration $\{\mathbf{R}\}$, where the spins fluctuate around the first axis:

$$\mathbf{R}_{n_B} = \begin{pmatrix} \sqrt{1 - \bar{\chi}_{n_B}^2} \\ \bar{\chi}_{n_B} \end{pmatrix}, \quad (13)$$

where $\bar{\chi}_{n_B}$ has two components, and $|\bar{\chi}_{n_B}| \ll 1$. For the

TABLE I. Couplings used for the parametrization of the FP action including instanton configurations. The graphical notation is explained in the text.

No.	Type	Coupling	Type	Coupling	Type	Coupling
1		0.61884		-0.04957		-0.00932
4		0.19058		-0.02212		-0.00746
7		0.01881		-0.00180		0.00658
10		0.02155		0.00536		-0.00081
13		0.00941		0.00488		-0.00225
16		0.01209		0.00534		0.00066
19		-0.00258		-0.00173		0.00146
22		-0.01040		-0.00218		0.02720

minimizing fine field we can make the ansatz

$$\mathbf{S}_n^{(1)} = \begin{pmatrix} \sqrt{1 - \vec{\pi}_n^2} \\ \vec{\pi}_n \end{pmatrix}. \quad (14)$$

Inserted in the FP equation, the above expansion leads in leading order to the free field case. This was solved by Bell and Wilson [18] (for a brief review see, for instance, Ref. [13]). Here we only report the relation between $\vec{\pi}_n$ and $\vec{\chi}_{n_B}$:

$$\vec{\pi}_n = \sum_{n_B} \alpha(n, n_B) \vec{\chi}_{n_B}. \quad (15)$$

Here α is given by

$$\alpha(n, n_B) = \int_0^{2\pi} \frac{d^2 q}{(2\pi)^2} e^{-iq(n-2n_B)} \frac{1}{4} \frac{\tilde{\rho}_{\text{FP}}(2q)}{\tilde{\rho}_{\text{FP}}(q)} \prod_{j=1}^2 \frac{1 - e^{-2iq_j}}{1 - e^{-iq_j}}, \quad (16)$$

where $\tilde{\rho}_{\text{FP}}(q)$ is the coefficient in the quadratic part of the FP action (given by the free field case). By iterating Eq. (15) one can obtain the FP field operator in the free field case. The form is very similar to the above result, but with slightly modified parameters [14].

On smooth configurations $\{\mathbf{R}\}$ Eqs. (13)–(15) give a good approximation. However, we want to evaluate the fine field using a parametrization that performs well not only for smooth configurations $\{\mathbf{R}\}$, but also for general ones. Our experience with the parametrization of the FP action suggests the ansatz

$$\mathbf{S}_n = \mathcal{N} \left[\sum_{n_B} \alpha(n, n_B) \mathbf{R}_{n_B} + \sum_{\substack{n_B \\ m_B, m'_B}} \beta(n, n_B, m_B, m'_B) \frac{1}{2} \vartheta_{m_B, m'_B}^2 \mathbf{R}_{n_B} \right], \quad (17)$$

where \mathcal{N} is a normalizing factor, which ensures $\mathbf{S}_n^2 = 1$. As for the action, we found it to be useful to replace the scalar product $(1 - \mathbf{R}_{m_B} \mathbf{R}_{m'_B})$ between the coarse spins at sites m_B and m'_B , respectively, by the angle $\frac{1}{2} \vartheta_{m_B, m'_B}^2$. In order to determine the coefficients β , we numerically minimized the FP equation (10) using 60 configurations with lattice size 5 as input and stored the resulting fine lattices. The coefficients were then determined by minimizing the difference between the minimized fine spins and the parametrization (17).

The numerical values of the coefficients α and β are given in Table II together with a symbolic notation of the corresponding operators. We chose a set of 23 operators mainly because of their compactness. Operators 1–6 are the analytically determined coefficients α , and 7–23 are the numerically determined coefficients β . The meaning of the graphical notation of the operators is the following: The dashed lines represent a 3×3 section of the coarse lattice grid. The cross $+$ in between indicates the position n of the fine spin \mathbf{S}_n in Eq. (17). The little square (\square) denotes the position n_B of the coarse spin \mathbf{R}_{n_B} . The two connected dots $\bullet \longrightarrow$ are the positions m_B and m'_B of the spins whose angle $\frac{1}{2} \vartheta_{m_B, m'_B}^2$ enters into the parametrization. Graphs obtained by trivial symmetry transformations are not drawn separately.

III. INSTANTONS

A. Instantons on the lattice

In infinite volume continuum field theory topology is a well-defined concept. Field configurations can be classified in topological sectors according to a “winding number” or topological charge [19]. In a lattice formulation this concept breaks down. When discretizing a theory, continuity in coordinate and internal space is lost. On the other hand, topology is based on continuous transformations of mappings, which are separable into classes. In a discretized theory every field configuration can be continuously transformed into any other. If lattice configurations are sufficiently smooth, an unambiguous topological charge may be assigned. Conversely, for field configurations containing large fluctuations, an interpolation is not unique, and a charge definition becomes ambiguous.

An additional problem arises due to the discretization of the continuum action. While the continuum action possesses scale-invariant instanton solutions, this is generally not true for discretized actions. In particular, starting with nonzero charged configurations, Lüscher [4] found that one can continuously lower the standard lattice action to zero by a local minimization in the spin

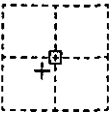
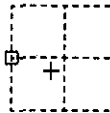
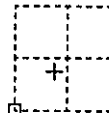
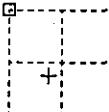
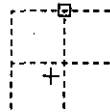
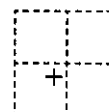
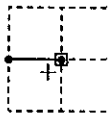
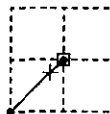
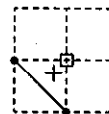
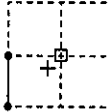
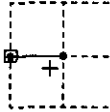
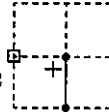
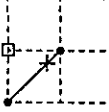
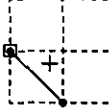
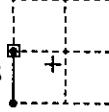
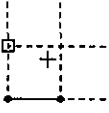
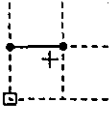
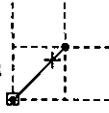
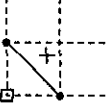
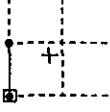
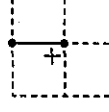
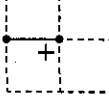
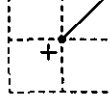
variables.

In Ref. [13] investigating the above problems with the aid of renormalization group methods was suggested, and it was shown that the FP action has scale-invariant instanton solutions. In this section we continue along these lines and construct instanton solutions of the FP action.

These in turn can be used to study the performance of a proposed improved topological charge definition. But first, let us review some basic facts about instantons in the continuum [19].

In an infinite volume, configurations with a finite action play a special role: At "infinity" all spin variables

TABLE II. Coefficients of the parameterization of the fine field.

No.	Type	Coeff.	No.	Type	Coeff.	No.	Type	Coeff.
1		0.59497	2		0.15621	3		0.08300
4		0.00942	5		-0.00171	6		-0.00668
7		-0.01228	8		-0.02004	9		-0.03832
10		-0.05095	11		0.01475	12		-0.00586
13		-0.00303	14		-0.00123	15		-0.00118
16		-0.01596	17		-0.00090	18		0.00140
19		-0.00128	20		0.00447	21		0.00199
22		0.00304	23		-0.00015			

point in the same direction, and the space \mathbf{R}^2 can be compactified by stereographic projection into a sphere S^2 . A finite action configuration is thus a mapping of a "coordinate" sphere onto the internal sphere $\mathbf{S}_n^2 = 1$. Such mappings can be classified by homotopy classes, with an integer number, the topological charge Q , characterizing the sectors. While configurations from the same topological sector can be continuously deformed into each other, this is not true for configurations with a different charge. The charge Q is the number of times the internal sphere is wrapped as the coordinate sphere is traversed. It may be defined as the integral

$$Q = \frac{1}{8\pi} \int d^2x \epsilon_{\mu\nu} \mathbf{S} \cdot (\partial_\mu \mathbf{S} \times \partial_\nu \mathbf{S}), \quad (18)$$

and it is related to the action by the inequality

$$\mathcal{A} \geq 4\pi |Q|. \quad (19)$$

If for a given configuration the equality is satisfied, the configuration minimizes the action and is therefore a solution of the equations of motion.

Let us now turn to the theory in a finite volume. By demanding periodic boundary conditions

$$\mathbf{S}(x_1 + Lm, x_2 + Ln) = \mathbf{S}(x_1, x_2), \quad \text{where } m, n \in \mathbb{Z} \quad (20)$$

we define the theory on a square torus of size L . In a finite volume every field configuration has a finite action, and because of the periodic boundary conditions an integer topological charge Q associated with it.

We can now explicitly construct pure instanton or pure anti-instanton configurations with an action $\mathcal{A} = 4\pi|Q|$ [20]. We use the plane coordinates defined by the stereographic projection to describe the solutions:

$$\begin{aligned} \mathbf{S}_i &= \frac{2u_i}{1+|u|^2}, & i &= 1, 2, \\ \mathbf{S}_3 &= \frac{1-|u|^2}{1+|u|^2}, \end{aligned} \quad (21)$$

where $u = u_1 + iu_2$. The instanton solutions at the boundary of Eq. (19) satisfy the Cauchy-Riemann equations for u being an analytic function in $z = x_1 + ix_2$:

$$(\partial_1 + i\partial_2)u = 0. \quad (22)$$

The solutions are doubly periodic meromorphic functions called elliptic functions [20]. They can be written as

$$u = c \prod_{i=1}^k \frac{\sigma(z - a_i)}{\sigma(z - b_i)} \quad \text{with} \quad \sum_{i=1}^k a_i = \sum_{i=1}^k b_i. \quad (23)$$

Here the integer k is the topological charge of the solution and c, a_1, \dots, a_k , and b_1, \dots, b_k are complex numbers. $\sigma(z)$ is the Weierstrass σ function with half periods $\omega = L/2$ and $\omega' = iL/2$. Using Cauchy's theorem one can

show that there are no solutions with a topological charge equal to one [20]. Hence we are forced to construct charge two instanton solutions. Specifically, we set $k = 2$ and $c = 1$. A reasonable definition for the instanton size is

$$\rho = \frac{1}{2} \min\{|a_1 - b_1|, |a_1 - b_2|\}. \quad (24)$$

Let us now turn to the construction of instanton solutions on the lattice. As was pointed out in Ref. [13], the FP action allows scale-invariant instanton solutions. Since we use this fact to construct instantons on the lattice, it is appropriate to repeat the statement:

If a given configuration $\{\mathbf{R}\}$ satisfies the equations of motion for the FP action \mathcal{A}_{FP} and it is a minimum, then the solution $\{\mathbf{S}\}$ of the FP equation (10) satisfies the equations of motion also. Moreover, both configurations yield the same value for the action.

The proof is quite simple. If $\{\mathbf{R}\}$ is at a local minimum of the FP action \mathcal{A}_{FP} , variations with respect to $\{\mathbf{R}\}$ will vanish:

$$\frac{\delta \mathcal{A}_{\text{FP}}(\mathbf{R})}{\delta \mathbf{R}_{n_B}} = \kappa \left[- \sum_{n \in n_B} \mathbf{S}_n + \mathbf{R}_{n_B} \left(\mathbf{R}_{n_B} \cdot \sum_{n \in n_B} \mathbf{S}_n \right) \right] = 0. \quad (25)$$

Here $\mathbf{S} = \mathbf{S}(\mathbf{R})$ is the solution of the FP equation with $\{\mathbf{R}\}$ as coarse input configuration. Since $\{\mathbf{R}\}$ is a local minimum, Eq. (25) implies

$$\mathbf{R}_{n_B} = \frac{\sum_{n \in n_B} \mathbf{S}_n}{|\sum_{n \in n_B} \mathbf{S}_n|}. \quad (26)$$

Consequently, we have

$$\mathcal{T}(\mathbf{R}, \mathbf{S}) = 0. \quad (27)$$

Since the transformation kernel $\mathcal{T}(\mathbf{R}, \mathbf{S}) \geq 0$, the configuration $\{\mathbf{S}\}$ gives its minimum for fixed $\{\mathbf{R}\}$. Because the configuration $\{\mathbf{S}\}$ minimizes the right-hand side of the FP equation, it minimizes the FP action $\mathcal{A}_{\text{FP}}(\mathbf{S})$ separately. Therefore it is a solution of the equations of motion. Since $\mathcal{T}(\mathbf{R}, \mathbf{S}) = 0$, both actions have the same value: $\mathcal{A}_{\text{FP}}(\mathbf{R}) = \mathcal{A}_{\text{FP}}(\mathbf{S})$. This concludes the proof.

The reverse of the above statement is, in general, not true for arbitrary configurations. Although a fine configuration, which is a solution of the FP equations of motion and which is used to construct a coarse configuration by means of the above blocking equation (26), locally minimizes the right-hand side of the FP equation, this minimum does not necessarily coincide with the absolute one. This, in fact, prevents the existence of arbitrary small instanton solutions.

Using the above ideas, it is clear how to construct instanton solutions of \mathcal{A}_{FP} . We naively discretize the continuum instanton solution on a very fine lattice with spacing $a_0 = 2^{-k}a$. After performing k blocking steps as defined by Eq. (26), we obtain a configuration $\{\mathbf{R}\}$ on a lattice with spacing a . In the limit $k \rightarrow \infty$, we recover the continuum solution, which is, of course, a local

minimum of the continuum action. Since all the successive blocked configurations minimize the transformation kernels in the iterated FP equation, the configuration $\{\mathbf{R}\}$ is a good candidate for a lattice solution of the FP action.¹ We may solve the FP equation for $\{\mathbf{R}\}$ to check whether it is still a solution. If $\{\mathbf{R}\}$ is a solution, then the multigrid minimization procedure should lead to the same configurations on finer lattices as those which were used in constructing $\{\mathbf{R}\}$ by blocking.

B. Definition of the topological charge on the lattice

In the following we define a topological charge operator based on the multigrid solution of the FP action. We evaluate the FP topological charge by means of the solutions of the FP equation (10). Under a RG transformation an operator $\mathcal{O}(\mathbf{S})$ transforms into $\mathcal{O}'(\mathbf{R})$ on the coarse lattice as

$$\mathcal{O}'(\mathbf{R})e^{-\beta A'(\mathbf{R})} = \int \mathcal{D}\mathbf{S} \mathcal{O}(\mathbf{S})e^{-\beta[A(\mathbf{S})+T(\mathbf{R},\mathbf{S})]}. \quad (28)$$

In the limit $\beta \rightarrow \infty$ the path integral on the right-hand side is approximated by its saddle point, and we obtain

$$\mathcal{O}'(\mathbf{R}) = \mathcal{O}(\mathbf{S}(\mathbf{R})), \quad (29)$$

where the spin configuration $\{\mathbf{S}(\mathbf{R})\}$ is the solution of the FP equation (10). Repeated application of this transformation will single out the operator with the largest eigenvalue. Since the topological charge is expected to be a marginal operator, we may obtain it as the limit

$$Q_{\text{FP}}(\mathbf{R}) = \lim_{k \rightarrow \infty} Q(\mathbf{S}^{(k)}(\mathbf{R})). \quad (30)$$

Here Q is some standard lattice charge definition and $\{\mathbf{S}^{(k)}\}$ is the solution of the iterated FP equation (11) on the lowest level in a k level multigrid (see Fig. 1). In other words, the FP topological charge is a standard topological charge evaluated on the FP field.

Note that $\mathbf{S}^{(k)}(\mathbf{R})$ becomes increasingly smooth as k grows: first, because the corresponding lattice spacing $a_0 = 2^{-k}a$ decreases, and second, because $\mathbf{S}^{(k)}(\mathbf{R})$ becomes almost a solution to the equations of motion. Consequently, any sensible definition of the topological charge can be used in these configurations; the final result will not depend on this choice. Nevertheless, it is more convenient to use the geometric definition, since it is stable against small variations of the field, and hence k , the number of levels in the multigrid minimization, could be kept small with this definition. For a review of the geometric definition, we refer the reader to Ref. [3].

One can easily show that with this definition of the topological charge there are no dangerous dislocations.

More precisely, one has

$$A_{\text{FP}}(\mathbf{R}) \geq 4\pi |Q_{\text{FP}}(\mathbf{R})|, \quad (31)$$

for arbitrary configuration $\{\mathbf{R}\}$. The corresponding statement is true in the continuum; hence, it is also true for $\mathbf{S}^{(k)}(\mathbf{R})$ for $k \rightarrow \infty$. Equation (31) follows then by observing that the contribution of the T terms in Eq. (10) is non-negative. We are now ready to discuss the numerical aspects of classical solutions.

C. Classical numerical results

Following the above program, we naively discretize two-instanton solutions on the torus of various sizes on very fine lattices. We find that four to five blocking steps are sufficient to make any lattice artifacts of the original discretization negligible. On the finally blocked configurations we can measure several quantities. On the coarse configuration itself we measure the standard action and the parametrization of the FP action presented in Sec. IIB. Performing a minimization on a multigrid with three finer levels, we measure the exact FP action and on the finest level the FP charge. Using the instanton radius given by Eq. (24), we get a parameter that well characterizes the breakdown of the blocking to obtain instanton solutions on coarse lattices: In Fig. 2 it can be clearly seen that below an instanton radius of $\rho \lesssim 0.7a$ the configurations are no longer instanton solutions, and we shall say that the instanton falls through the lattice. It is gratifying to see that the FP charge immediately falls off to zero, as the FP action drops below the continuum value. Furthermore, Fig. 2 demonstrates how well the parametrization for the FP action is suited for instanton configurations. The deviation from the exact value is quite small, in particular the parametrized FP action is only marginally smaller than the continuum value in the region above the point where the instanton falls through the lattice. In contrast, the values of the standard action

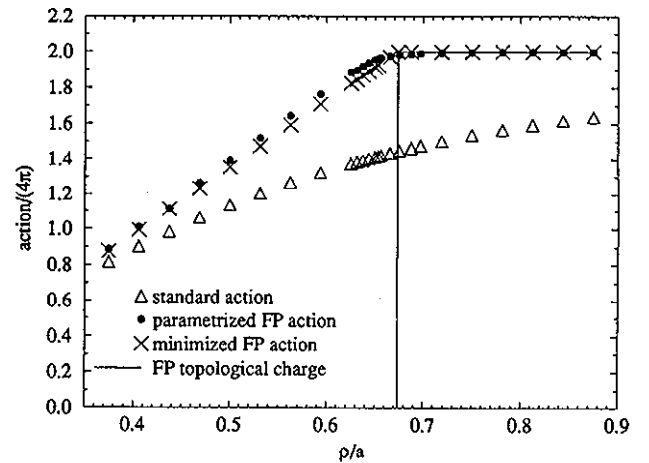


FIG. 2. Actions and charge of instantons with radii of the order of one lattice spacing.

¹It will be a solution, unless the size of the instantons is too small with respect to the lattice spacing.

are quite different from the continuum ones. These numerical findings support the above statement, that there are no dangerous dislocations present when using the FP action together with the FP topological charge.

In numerical simulations we use a parametrized form of the FP action and the parametrization in Eq. (17) for the FP field instead of the time consuming minimization procedure. One then is interested as to whether the use of these two parametrizations has an influence on the existence of dislocations. The curves referring to the FP action and FP charge in Fig. 2 have a nonanalytic break at $\rho/a \simeq 0.7$. Our parametrization does not fully reproduce this behavior, and so one might expect that observable deviations will occur in this instanton region. We systematically searched for minimal action configurations with a parametrized action lower than the continuum value in the $Q_{\text{FP}}^{\text{par}} = 2$ sector. We find a minimal action of $1.84 \times 4\pi$ (compare this with the value $0.93 \times 4\pi$ that we find using the standard action and geometric charge). This value can be ascribed to the not exactly accurate parametrization of the FP field. If we actually solve the FP equation (10) for this “dislocation configuration” we get the correct charge $Q = 0$. Nevertheless, as one has to use parametrizations for Monte Carlo simulations, such configurations could be dangerous. On the other hand, the search for dislocations reveals the weakest point of the parametrization that performs very well in other cases (cf. Fig. 2). What actually counts is not how the parametrization works for some configurations that were specially sought for their bad performance, but how well it performs for configurations in thermal equilibrium occurring in a Monte Carlo simulation. The results of a test of this performance, presented in Sec. IV A, shows that indeed there is no problem.

We also searched for the minimal action configuration in the $Q = 1$ sector and did not find a configuration with an action below the continuum action. This is not astonishing as there are no one-instanton solutions on a torus.

IV. TOPOLOGICAL SUSCEPTIBILITY

If the topological susceptibility is a well-defined physical quantity that is renormalization-group invariant, then one expects that it scales like a $(\text{mass})^2$ in the continuum limit. One additionally measures a second quantity, e.g., the correlation length ξ , and builds the dimensionless

product $\chi_t \xi^2$, which should go to a constant in the limit $\xi \rightarrow \infty$. Earlier Monte Carlo calculations do not show convincingly whether this is the case. Furthermore, perturbative considerations indicate that in the $O(3)$ model there might be a problem with the topological susceptibility in the continuum limit.

One may calculate the contribution of instantons in the continuum using a semiclassical expansion. The probability density to find an instanton with topological charge $Q = 1$ and size $\rho \ll 1/\Lambda$ is [21,22]

$$P_1 \sim \frac{d\rho}{\rho}, \quad (32)$$

where Λ is the scale parameter of the model. Using the renormalization group, one can show that Eq. (32) is exact as $\rho \rightarrow 0$ [4] assuming the small instantons form a dilute gas. The ultraviolet divergence at $\rho = 0$ in Eq. (32) indicates, however, that this assumption is not true: Small instantons are not suppressed but contribute strongly to the susceptibility. Such a dominance of small instantons is also indicated by numerical studies, trying to determine the instanton size distribution with different methods [11,12].

On the lattice, however, not the whole range of the instanton radius is probed. The lattice cuts the contribution of small instantons because there is a smallest possible radius before the instanton falls through the lattice (cf. Fig. 2). Hence the measured topological susceptibility is always finite. It is not excluded, however, that it raises boundlessly with increasing correlation length as the perturbative considerations suggest.

Using the perfect lattice action and the perfect charge, we performed extensive Monte Carlo simulations at correlation lengths in the range $\xi \in (2 - 60)$. In order to avoid finite size effects, we kept the ratio $L/\xi \approx 6$ constant. The correlation length was obtained from the long-distance behavior of the zero space momentum correlation function.

We determined the topological charge using both the geometric definition and the definition of the FP charge given in Sec. III B. For the measurement of the FP charge, we used the geometric definition of the charge on a finer lattice of the multigrid with the Monte Carlo generated lattice as coarsest level. To determine the configuration $\mathbf{S}(\mathbf{R})$ on the fine lattice, one can either minimize the FP equation (which is very time consuming) or use the parametrization of the dependence on \mathbf{R} given in Sec. II C. We denote the corresponding charges Q_{coarse}

TABLE III. Results of test MC simulations in the $O(3)$ model indicating that it is sufficient to measure the charge only on the first finer parametrized level. Minimizing or going to a lower level yields the same result.

β	$\langle Q_{\text{coarse}}^2 \rangle$	$\langle Q_{\text{par 1st level}}^2 \rangle$	$\langle Q_{\text{par 2nd level}}^2 \rangle$	$\langle Q_{\text{min 1st level}}^2 \rangle$	$\langle Q_{\text{min 2nd level}}^2 \rangle$
0.6	2.56(5)	1.96(4)	1.93(4)		
0.7	3.39(4)	2.48(3)	2.45(3)	2.45(3)	2.45(3)
0.85	5.62(11)	4.31(9)	4.30(9)		
1.0	6.38(8)	4.86(6)	4.82(6)		
1.0	6.33(6)	4.78(5)		4.75(5)	

TABLE IV. Results of MC simulations with the FP action.

β	L	ξ	$\langle Q_{\text{coarse}}^2 \rangle$	$\chi_{\text{coarse}}^t \cdot \xi^2$	$\langle Q_{\text{1st level}}^2 \rangle$	$\chi_{\text{1st level}}^t \cdot \xi^2$
0.51	10	1.6049(42)	1.87(1)	0.0482(4)	1.329(8)	0.0342(3)
0.6	14	2.1960(46)	2.57(2)	0.0631(6)	1.90(2)	0.0467(4)
0.685	20	3.012(14)	3.57(3)	0.0810(10)	2.65(2)	0.0601(7)
0.7	20	3.186(15)	3.36(3)	0.0852(11)	2.52(2)	0.0640(8)
0.85	40	6.057(17)	5.73(4)	0.1314(12)	4.38(3)	0.1004(9)
1.0	70	12.156(34)	6.36(5)	0.1918(19)	4.80(4)	0.1448(15)
1.1	130	20.397(86)	10.04(12)	0.2472(36)	7.69(9)	0.1893(27)
1.2	180	34.44(30)	8.23(14)	0.3013(73)	6.11(10)	0.2237(53)
1.3	340	58.06(37)	12.01(29)	0.3502(96)	8.94(22)	0.2607(72)

for the geometric charge, $Q_{\text{par 1st level}}$ for the charge measured on the first finer level using the parametrization of the fine field, etc.

For two β values, we compared the results of using the parametrization on a finer level and of minimizing on a multigrid. As is shown in Table III, the results were found to be consistent within the statistical errors. This confirms that the parametrization performs well for configurations occurring in a Monte Carlo simulation (cf. the discussion at the end of Sec. III C). In order to test if the result of going to a lower level is already stable, we also calculated the charge for a few β values on the second finer lattice. As also can be seen in Table III, the values on the first and the second finer level were found to be consistent within the statistical errors. Thus it is sufficient to calculate the fine field only on the first finer level. This is not astonishing as the maximal angle between two neighboring spins halves as one goes one step down to a finer level. So even on the first finer level the maximal possible angle between two neighboring spins is 90° , and there is practically no ambiguity left for the topological charge.

In Table IV we report the results of the simulations for the correlation length ξ , the geometric charge $\langle Q_{\text{coarse}}^2 \rangle$ and the FP charge $\langle Q_{\text{1st level}}^2 \rangle$ evaluated on the first parametrized finer level. Using the geometric charge as

well as the FP charge, we build the dimensionless quantity $\chi^t \cdot \xi^2$ of topological susceptibility and correlation length.

Figure 3 shows the results for the topological susceptibility. Clearly, no scaling is seen even at correlation lengths as large as 60. Both curves, the one for the geometric charge and the one for the FP charge, are rising, and no flattening occurs at the largest correlation lengths. There is a significant difference between the topological susceptibility built with the geometric charge and the one with the FP charge. The value of the geometric charge lies several standard deviations above the value of the FP charge. Furthermore, the difference is slowly growing with increasing correlation length.

V. CONCLUSION AND OUTLOOK

The definition of the FP topological charge is based on the FP field operator. The FP field can be evaluated to any precision desired by solving the iterated FP equation on a k level multigrid. As was demonstrated by Fig. 2 and can be shown analytically for sufficient large multigrids, the FP charge together with the FP action has no lattice defects whatsoever.

For use in MC simulations, however, a parametrization of the action and the charge are needed. Instead of parametrizing the charge directly, we have parametrized the solution of the FP equation, which is to be iterated to obtain the FP field. The accuracy of the parametrizations have been rechecked in MC simulations.

The partition function of the lattice σ model is, as indicated by a semiclassical approximation [21], dominated by small sized topological excitations. These fluctuations are the cause for the divergence, which is seen in Fig. 3.

Although we studied the σ model in this paper, the methods derived are quite general and can be applied to other asymptotically free theories such as CP^{N-1} models or $SU(N)$ gauge models. For instance, in CP^{N-1} models a lowest-order semiclassical approximation estimates for instanton contributions [21,22]

$$I \sim \int d\rho \rho^{N-3}. \quad (33)$$

If $N \geq 4$, the contribution of short-distance topological

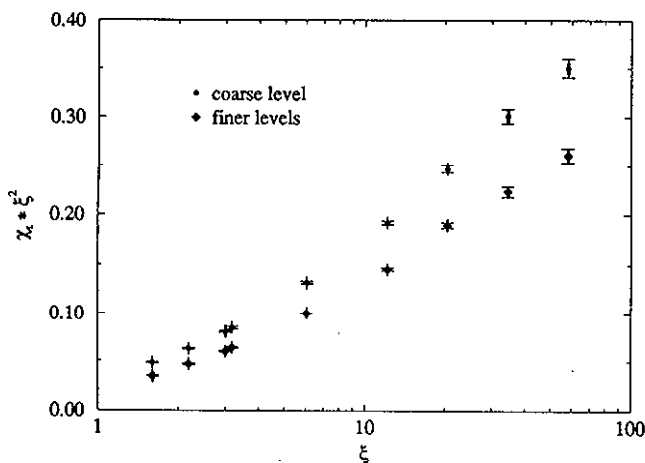


FIG. 3. Results of Monte Carlo measurements of the topological susceptibility at different correlation lengths.

excitations is small relative to that of the physical ones, and we expect to see a scaling of the topological susceptibility according to the perturbative RG. In fact, in the CP^3 model, which is studied by one of us [17], the topological susceptibility already exhibits the expected scaling behavior.

ACKNOWLEDGMENTS

We wish to thank T. DeGrand, A. Hasenfratz, A. Papa, and U. Wiese for useful discussions. This work was supported in part by Schweizerischer Nationalfonds.

-
- [1] S. Weinberg, *Phys. Rev. D* **11**, 3583 (1975); G. 't Hooft, *ibid.* **14**, 3432 (1976); *Phys. Rev. Lett.* **37**, 8 (1976).
 - [2] E. Witten, *Nucl. Phys.* **B156**, 269 (1979); G. Veneziano, *ibid.* **B159**, 213 (1979).
 - [3] B. Berg and M. Lüscher, *Nucl. Phys.* **B190**[FS3], 412 (1981).
 - [4] M. Lüscher, *Nucl. Phys.* **B200**[FS4], 61 (1982).
 - [5] B. Berg, *Phys. Lett.* **104B**, 475 (1981); *Nucl. Phys.* **B251**[FS13], 353 (1985).
 - [6] P. DiVecchia, K. Fabricius, G.C. Rossi, and G. Veneziano, *Nucl. Phys.* **B192**, 392 (1981); K. Ishikawa, G. Schierholz, H. Schneider, and M. Teper, *Phys. Lett.* **128B**, 309 (1983).
 - [7] M. D'Elia, F. Farchioni, and A. Papa, *Nucl. Phys.* **B456**, 313 (1995).
 - [8] M. Teper, *Phys. Lett. B* **232**, 227 (1989).
 - [9] A. Di Giacomo, F. Farchioni, A. Papa, and E. Vicari, *Phys. Rev. D* **46**, 4630 (1992).
 - [10] M. Teper, *Phys. Lett. B* **171**, 81 (1986); **171**, 86 (1986); *Nucl. Phys. B (Proc. Suppl.)* **20**, 159 (1991).
 - [11] C. Michael and P.S. Spencer, Report No. LTH-328, hep-lat/9401011 (unpublished); *Phys. Rev. D* **50**, 7570 (1994).
 - [12] F. Farchioni and A. Papa, *Nucl. Phys.* **B431**, 686 (1994).
 - [13] P. Hasenfratz and F. Niedermayer, *Nucl. Phys.* **B414**, 785 (1994).
 - [14] T. DeGrand, A. Hasenfratz, P. Hasenfratz, and F. Niedermayer, *Nucl. Phys.* **B454**, 587 (1995).
 - [15] T. DeGrand, A. Hasenfratz, P. Hasenfratz, and F. Niedermayer, *Nucl. Phys.* **B454**, 615 (1995); some results were presented by T. DeGrand, A. Hasenfratz, P. Hasenfratz, F. Niedermayer, and U.J. Wiese, *Nucl. Phys. B (Proc. Suppl.)* **42**, 67 (1995).
 - [16] M. Blatter, R. Burkhalter, P. Hasenfratz, and F. Niedermayer, *Nucl. Phys. B (Proc. Suppl.)* **42**, 799 (1995).
 - [17] R. Burkhalter, Report No. BUTP-95/18 (unpublished).
 - [18] T.L. Bell and K. Wilson, *Phys. Rev. B* **10**, 3935 (1974).
 - [19] A.A. Belavin and A.M. Polyakov, *JETP Lett.* **22**, 245 (1975); A.M. Polyakov, *Gauge Fields and Strings* (Harwood, Chur, 1987); R. Rajaraman, *Solitons and Instantons* (North-Holland, Amsterdam, 1982).
 - [20] J.-L. Richard and A. Rouet, *Nucl. Phys.* **B211**, 447 (1983); A. Erdélyi, W. Magnus, F. Oberhettinger, and F.G. Tricomi, *Higher Transcendental Functions* (McGraw-Hill, New York, 1953), Vol. 2.
 - [21] A. Jevicki, *Nucl. Phys.* **B127**, 125 (1977); D. Förster, *ibid.* **B130**, 38 (1977); V.A. Fateev, I.V. Frolov, and A.S. Schwarz, *ibid.* **B154**, 1 (1979); B. Berg and M. Lüscher, *Commun. Math. Phys.* **69**, 57 (1979).
 - [22] P. Schwab, *Phys. Lett.* **118B**, 373 (1982); **126B**, 241 (1983); M. Lüscher, *Nucl. Phys.* **B205**[FS5], 483 (1982).